JOURNAL OF VIROLOGY, Mar. 2005, p. 2709–2719 Vol. 79, No. 5
0022-538X/05/$08.00+0 doi:10.1128/JVI.79.5.2709–2719.2005

Early Antiretroviral Therapy for Simian Immunodeficiency Virus Infection Leads to Mucosal CD4$^+$ T-Cell Restoration and Enhanced Gene Expression Regulating Mucosal Repair and Regeneration

Michael D. George, Elizabeth Reay, Sumathi Sankaran, and Satya Dandekar*

Department of Medical Microbiology and Immunology, University of California, Davis, Davis, California

Received 10 September 2004/Accepted 10 November 2004

Simian immunodeficiency virus (SIV) and human immunodeficiency virus (HIV) infections lead to rapid depletion of CD4$^+$ T cells from gut-associated lymphoid tissue (GALT). Although the administration of antiretroviral therapy (ART) has been shown to increase CD4$^+$ T-cell levels in the peripheral blood in both SIV and HIV infections, its efficacy in restoring intestinal mucosal CD4$^+$ T cells has not been well investigated. To gain insights into the molecular mechanisms of virally induced disruptions in the mucosal immune system, we have evaluated longitudinal changes in viral burden, T-cell subsets, and mucosal gene expression profiles in SIV-infected rhesus macaques in the absence or presence of ART. Our results demonstrate a dramatic suppression of mucosal viral loads and rapid reconstitution of CD4$^+$ T cells in GALT in animals receiving ART that were not observed in untreated SIV-infected animals. DNA microarray-based gene expression profiling indicated that CD4$^+$ T-cell restoration in GALT was associated with up regulation of growth factors and genes involved in repair and regeneration of the mucosal epithelium. In contrast, untreated SIV-infected animals increased expression of lymphocyte activation and inflammatory response-associated genes and did not up regulate mucosal growth and repair associated transcription. In conclusion, these data indicate that initiating ART in primary SIV infection may lead to the restoration of the mucosal immune system through reduction of inflammation and promotion of epithelial repair in the intestinal mucosa.

Both simian immunodeficiency virus (SIV) and human immunodeficiency virus (HIV) infections lead to dysregulation of T-cell homeostasis in intestinal mucosal lymphoid tissue. Previous studies of SIV-infected rhesus macaques have demonstrated that intestinal mucosal CD4$^+$ T cells are severely depleted early in primary SIV infection (4, 11, 12, 15, 29, 39). Recently, it was discovered that dramatic CD4$^+$ T-cell depletion also occurs in gut lymphoid tissue of humans during primary HIV type 1 (HIV-1) infection (6). In both HIV and SIV infections, intestinal CD4$^+$ T-cell depletion coincided with characteristic increases in CD8$^+$ T-cell percentages (4, 6, 15, 18, 28, 29, 38, 40) and proinflammatory markers (19, 25). Additionally, increased levels of apoptosis, mucosal enteropathy, and nutrient malabsorption have been reported in acute and chronic stages of both SIV and HIV infections (1, 7, 8, 11–14, 20, 27, 35, 41). These studies support the hypothesis that disruption of mucosal T-cell homeostasis and increased inflammatory responses in gut-associated lymphoid tissue (GALT) during primary stage infection may lead to ineffective local immune responses, impaired mucosal epithelial barrier and absorptive functions, and reduced regenerative capacity.

Antiretroviral therapy (ART) leads to suppression of plasma viral burden and increased CD4$^+$ T-cell numbers in peripheral blood during both HIV-1 and SIV infections (2, 9, 26, 30, 31, 32, 34, 36, 37). Interestingly, initiation of highly active antiviral therapy (HAART) during primary HIV-1 infection was recently shown to result in CD4$^+$ T-cell restoration in both gut lymphoid tissue and peripheral blood, while initiation of therapy during chronic infection resulted in delayed and incomplete CD4$^+$ T-cell repopulation (6). Studies in the SIV model indicate that, although CD4$^+$ T cells that repopulate the intestinal mucosa during antiviral therapy are activated, they may have a reduced capacity to produce interleukin-2 (IL-2) in response to mitogenic stimulation (16). Although the correlation between reduction in viral burden and repopulation of CD4$^+$ T cells during therapeutic intervention has been encouraging, the in vivo alterations in mucosal immune responses resulting from severe depletion and subsequent repopulation of CD4$^+$ T cells have not been fully characterized in either humans or nonhuman primates.

High-throughput DNA microarray-based gene expression analysis provides a powerful in vivo approach to comprehensively identify orchestrated changes in transcription in lymphoid tissue that result from SIV or HIV-1 infection and antiviral therapy (4, 6, 23). Because changes in the expression of thousands of genes can be assayed simultaneously, high-density microarray analyses offer functional assessment of multiple, and often interrelated, physiological pathways. Recently, in vivo gene expression studies have demonstrated that disruption of T-cell homeostasis in GALT during primary SIV infection coincided with increases in the expression of innate, cell-mediated, and humoral immune response factors, up regulation of apoptosis and necrosis-associated gene products, and down regulation of growth factors (4). Results from this study indicated that impaired mucosal regeneration may con-

* Corresponding author. Mailing address: Department of Medical Microbiology and Immunology, University of California, Davis, Davis, CA 95616. Phone: (530) 752-3409. Fax: (530) 752-8692. E-mail: sdandekar@ucdavis.edu.

tribute to acute enteropathy syndrome. Another report profiling host gene expression in lymph nodes of HIV-1-infected patients prior to and after receiving HAART indicated similar changes in gene expression and further suggested that inflammation and lymphocyte activation may be major contributors to HIV-1-induced tissue pathology in the absence of therapy (23). Alterations in host gene expression in GALT that are induced by chronic SIV infection and administration of antiretroviral therapy, however, remain unknown.

To gain insights into the in vivo effects of chronic SIV infection and ART on mucosal lymphocyte subset distribution and functional gene expression, we performed longitudinal analyses of viral burden, T-cell subsets, and host mucosal mRNA levels in SIV-infected rhesus macaques in the presence or absence of therapy. Our results indicated that, in contrast to ART-naïve SIV-infected macaques, (R)-9-(2-phosphonylmethoxypropyl)adenine (PMPA)-treated SIV-infected animals displayed significant viral suppression, restoration of intestinal and peripheral $CD4^+$ T cells, and a characteristic expression profile in GALT involving lymphocyte activation and inflammatory responses, as well as epithelial repair and regeneration.

MATERIALS AND METHODS

Animal subjects, infection, and tissue collection. Eight healthy, 3- to 4-year-old, colony-bred male rhesus macaques from the California National Primate Research Center were intravenously infected with 1,000 50% tissue culture infective doses ($TCID_{50}$) of SIV_{mac251} cells grown in peripheral blood mononuclear cells (PBMC). At 6 weeks postinfection (p.i.), five macaques were given antiviral therapy consisting of daily subcutaneous administrations (30 mg/kg of body weight) of PMPA, while the remaining three macaques received no antiretroviral treatment. Longitudinal samples of peripheral blood and jejunal biopsies were obtained prior to infection and again at 2, 6, 10, and 16 weeks p.i. Jejunal biopsies were obtained by upper endoscopy. Animals were necropsied at 26 weeks p.i., at which time peripheral blood and jejunum samples were obtained. Peripheral blood samples were analyzed for plasma viral loads by real-time PCR and immunophenotypic changes in circulating T-cell subsets by flow cytometry as described below. Jejunal biopsy samples were subjected to T-cell immunophenotypic analysis, immunohistochemical staining, quantitative real-time PCR assays, and DNA microarray analysis of host gene expression as described below.

Flow cytometry. Jejunal biopsies were incubated in RPMI 1640 medium (Invitrogen, Carlsbad, Calif.) and collagenase (Sigma, The Woodlands, Tex.) at 37°C for 45 min and subjected to a Percoll (Sigma) density gradient centrifugation to enrich for T cells and to eliminate tissue debris. Three-color flow cytometric analysis was performed to determine the percentages of $CD4^+$ and $CD8^+$ T cells by staining the cells with CD3FITC, CD4PE (BD Pharmingen, San Diego, Calif.), and CD8TC (Caltag, Burlingame, Calif.) as described previously (4). Cells were fixed in 1% paraformaldehyde–phosphate-buffered saline (PBS) and analyzed using a Becton Dickinson FACScan and CellQuest software (Becton Dickinson). Statistical analyses (Student's t test) were used to determine if differences in the mean values for uninfected and infected groups (untreated and PMPA treated) were significant ($P < 0.05$).

Real-time PCR. Plasma and jejunal biopsy samples were subjected to real-time PCR analyses to determine viral burden and changes in host gene expression. Briefly, primers and probes specific to the SIV RNA sequence or to human gene sequences for RANTES, MIP-1β, and granzyme A were designed and used in real-time PCRs as previously described (4). Fluorescent signal was detected with an ABI Prism 7700 sequence detector (PE Applied Biosystems). Data were captured and analyzed with Sequence Detector software (SDS). Viral copy number in plasma was determined by plotting C_T values (the fractional cycle number at which the fluorescence passes the fixed threshold for detection) against a standard curve derived from samples with known SIV copy numbers. In jejunal tissue samples, relative SIV viral RNA loads were calculated utilizing internal normalization of C_T values to the housekeeping genes glyceraldehyde-3-phosphate dehydrogenase (GAPDH) and 18S rRNA. Relative fold increases were determined by comparison of C_T values to the highest normalized C_T value (lowest copy number). Data were plotted as mean fold increases for PMPA-treated and untreated SIV-infected groups ± the standard error.

For host gene expression studies, internal normalization of C_T values was performed based on the housekeeping genes GAPDH and 18S rRNA, and differential gene expression was calculated by comparison of mean C_T values obtained from SIV-infected groups to the mean C_T values from four healthy uninfected controls. Statistical analyses (Student's t test) were used to determine if differences in the mean values for uninfected and infected groups (untreated and PMPA treated) were significant ($P < 0.05$).

Immunohistochemistry. Immunohistochemistry was performed to determine the number of $CD8^+$ T cells and the level of immunoglobulin G (IgG)-positive cells in jejunal tissue samples. Briefly, freshly isolated tissue samples were flash frozen in optimal cutting temperature embedding medium blocks. The tissue sections were then incubated with either anti-CD3 polyclonal antibody (Dako, Glostrup, Denmark), anti-CD8 polyclonal antibody (Dako), or anti-IgG monoclonal antibody (Santa Cruz Biotechnology, Santa Cruz, Calif.) at room temperature, followed by incubation with biotinylated secondary antibody and avidin-biotin-peroxidase complexes (LSAB II; Dako) and staining with 3,3 diaminobenzidine (Dako) as the chromogen. The tissue sections were washed and counterstained with hematoxylin, and coverslips were mounted with Permount (Fisher).

The $CD3^+$ and $CD8^+$ T cells in the lamina propria were counted both by computer analysis (Image J digital imaging software; National Institutes of Health, Bethesda, Md.) and manually in serial jejunum sections to provide additional quantitative analysis of changes in overall T-cell cellularity during treated and untreated SIV infection. Cells were counted in 10 well-oriented villi from each macaque, with the final data presented as the average cells per square millimeter ± the standard deviation. To determine gross structural changes, villus length and crypt depth in 10 well-oriented villi were measured with a cytometer as described previously (21). Average villus/crypt ratios for untreated and PMPA-treated SIV-infected macaques were compared to each other and to the ratio in uninfected healthy controls.

Microarray analysis. Gene expression profiles in jejunum samples from rhesus macaques were determined as previously described (4). RNA extractions, hybridization to U133A human GeneChips (Affymetrix, Santa Clara, Calif.), staining, and scanning were performed as described in the Affymetrix Expression Analysis Technical Manual. Total RNA was extracted from cryopreserved jejunum tissue samples utilizing the RNeasy RNA extraction kit (QIAGEN, Valencia, Calif.). Fluorescence intensity values (*.CEL files generated from Microarray suite 5.0) from scanned GeneChips were subjected to comparative analyses utilizing R statistical software (version 1.71) and BRB Array Tools (version 3.1; developed by Richard Simon and Amy Peng). Alterations in the amount of mRNA of any gene were reported only when (i) the change in expression was statistically significant ($P < 0.05$), (ii) the change was at least 50% (equivalent to a 1.5-fold change where the value for no change is 1) above or below the baseline transcription level (baseline = mean expression level in jejunum samples from six healthy, uninfected macaques), and (iii) the change occurred in a majority of macaques in the treated and/or untreated experimental groups (to ensure that a large change in a single animal did not account for the group observation). While it may be reasonable to assume that small changes (<50%) in expression of some of the genes may be sufficient to induce in vivo physiological changes in a cell or tissue, we chose a 50% change in expression to focus our analysis on profiling the genes that were most altered. K-means clustering (Spotfire, Decision Site version 1.0) was performed on genes whose expression changed according to the criteria described above to allow identification of similar patterns of regulated transcription. Statistically overrepresented biological processes within each K-means cluster were then identified using EASE version 1.0 analysis software (10). Genes with significant transcriptional changes involved in overrepresented pathways were further evaluated within the context of biological pathway maps (BioCarta; http://www.biocarta.com), as shown in Fig. 8, to consider the potential effects of their regulation on intestinal mucosal function.

RESULTS

Mucosal viral burden is dramatically reduced in SIV-infected macaques receiving antiviral therapy. To determine the effects of antiviral therapy on suppression of SIV replication, viral loads were measured at 2, 6, 10, 16, and 26 weeks p.i. in eight SIV-infected rhesus macaques. Antiviral therapy was initiated at 6 weeks p.i. in five of these macaques. As shown in Fig. 1A, peak plasma viral burden was detected at 2 weeks p.i.,

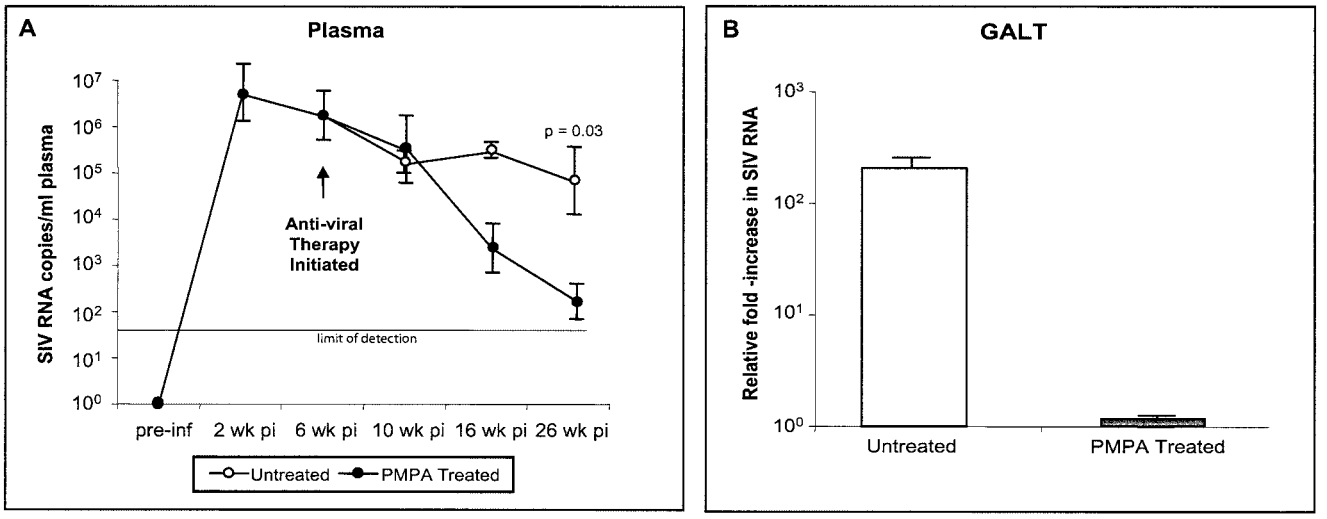

FIG. 1. Viral suppression in peripheral and mucosal compartments of SIV-infected macaques receiving ART. (A) Plasma compartment. Plasma viral loads were determined at 2, 6, 10, 16, and 26 weeks post-SIV infection in PMPA-treated (closed circles) and untreated (open circles) animals by real-time PCR. *P* values were calculated by using Student's *t* test. (B) GALT. Viral loads in GALT were determined at 26 weeks p.i. by real-time PCR. Relative fold changes were calculated by comparison of SIV RNA levels to the lowest level of SIV RNA measured in the PMPA-treated SIV-infected macaques.

which was followed by a modest decline at 6 weeks p.i. Although no significant difference in plasma viral loads was observed between the PMPA-treated and untreated groups following 4 weeks of therapy, a substantial reduction in viral loads was seen at 10 weeks posttherapy. After 20 weeks of therapy, the mean viral load was <200 copies/ml of plasma in treated animals, compared to $\sim 10^5$ copies/ml in untreated macaques. Statistical analysis (Student's *t* test) indicated that the difference in mean viral loads between treated and untreated macaques was significant ($P = 0.030$).

A dramatic difference in SIV burden in GALT was observed between PMPA-treated and untreated animals at 26 weeks p.i. (Fig. 1B). Untreated SIV-infected macaques, on average, displayed a relative 200-fold increase in SIV copy number above that detected in animals receiving ART. This observation was further supported by in situ hybridization analysis of SIV-infected cells in jejunum tissues (data not shown). Taken together, our data indicated that initiation of therapy during primary infection was effective at reducing viral burden in both peripheral and mucosal compartments.

Initiation of ART in primary SIV infection leads to efficient restoration of mucosal CD4$^+$ T cells. To evaluate the effect of initiating ART during primary SIV infection on restoration of intestinal mucosal immune system, we determined the prevalence of CD4$^+$ and CD8$^+$ T cells in longitudinal samples of jejunum and peripheral blood by flow cytometry. Mucosal CD4$^+$ T cells were depleted more rapidly and severely compared to peripheral CD4$^+$ T cells during primary SIV infection (Fig. 2A and B). Initiation of ART resulted in a steady increase in the prevalence of CD3$^+$/CD4$^+$ T cells in both mucosal and peripheral blood compartments. In contrast, severe mucosal CD4$^+$ T-cell depletion persisted in untreated SIV-infected animals. Individually, four of the five macaques receiving ART had restored mucosal CD4$^+$ T cells to >80% of preinfection levels following 20 weeks of therapy, and three of the five displayed >95% restoration (Fig. 2C), indicating that, in most animals, the initiation of ART during primary stage SIV infection led to nearly complete CD4$^+$ T-cell restoration in intestinal mucosa.

Decreased CD8$^+$ T lymphocytosis in GALT of PMPA-treated SIV-infected macaques. As observed in previous studies (4), SIV infection led to a rapid increase in the prevalence of CD8$^+$ T cells in intestinal mucosa and peripheral blood by 2 weeks p.i. The number of CD8$^+$ T cells in peripheral blood declined to near preinfection levels at 6 weeks p.i. and fluctuated only slightly thereafter (Fig. 3A). In contrast, intestinal CD8$^+$ T-cell levels remained elevated (>85% of CD3$^+$ T cells) in untreated animals. Initiation of ART in primary SIV infection led to a gradual decline (~65% of CD3$^+$ T cells) in mucosal CD8$^+$ T-cell levels.

To determine if the elevation in CD8$^+$ T-cell levels was due to a true increase in numbers or simply a compensatory effect of CD4$^+$ T-cell depletion, we examined the prevalence of mucosal CD8$^+$ T cells by immunohistochemistry. A marked increase in the number of CD8$^+$ T cells at 26 weeks p.i. was observed (Fig. 3C) in jejunal mucosa of untreated SIV-infected macaques (panel a) in comparison to macaques receiving ART (panel b) and healthy uninfected controls (panel c). Direct counting of the CD8$^+$ T cells detected in lamina propria indicated that untreated SIV-infected macaques had an average of 3,713 (± 1074) CD8$^+$ T cells/mm^2, while PMPA-treated SIV-infected animals had 1,741 (± 568) CD8$^+$ T cells/mm^2. Immunohistochemical analysis of CD3$^+$ T cells showed an overall increase (~30%) in GALT of all SIV-infected animals in comparison to uninfected controls (data not shown). No statistically significant difference, however, was observed in CD3$^+$ T-cell numbers between PMPA-treated and untreated SIV-infected animals.

Histopathological analysis indicated that PMPA-treated animals had an increased number of goblet cells (Fig. 3C, panel

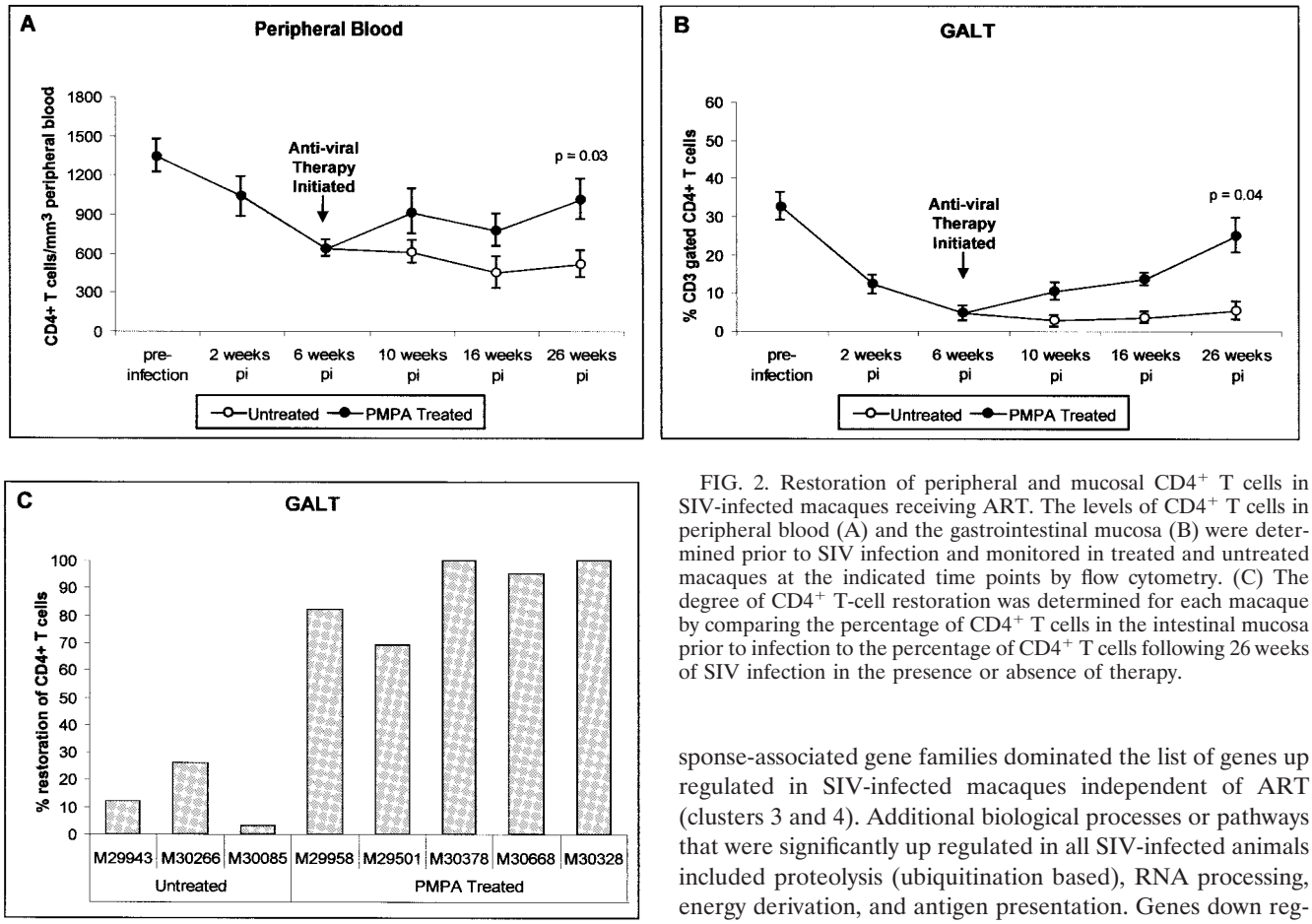

FIG. 2. Restoration of peripheral and mucosal $CD4^+$ T cells in SIV-infected macaques receiving ART. The levels of $CD4^+$ T cells in peripheral blood (A) and the gastrointestinal mucosa (B) were determined prior to SIV infection and monitored in treated and untreated macaques at the indicated time points by flow cytometry. (C) The degree of $CD4^+$ T-cell restoration was determined for each macaque by comparing the percentage of $CD4^+$ T cells in the intestinal mucosa prior to infection to the percentage of $CD4^+$ T cells following 26 weeks of SIV infection in the presence or absence of therapy.

b) in their villi in comparison to untreated animals and uninfected controls. Comparisons of the villus height and crypt depth ratio indicated no statistically significant difference among healthy uninfected controls and SIV-infected animals (data not shown), suggesting that the onset of histopathologic changes in the intestinal mucosa were not readily detectable within the first 26 weeks of infection.

Intestinal mucosal gene expression profiling in SIV-infected macaques. Differences in the restoration of the mucosal immune system in SIV-infected animals in the presence or absence of therapy provided a strong rationale for utilizing high-throughput gene expression studies to elucidate the molecular characteristics of their divergent phenotypes. Changes in mucosal gene expression were determined by comparing mRNA levels in jejunum tissue samples from healthy uninfected macaques ($n = 6$) and SIV-infected macaques ($n = 8$) by oligonucleotide microarray analysis. At 26 weeks p.i., we found statistically significant changes in the expression of 1,185 genes relative to their baseline level of expression in uninfected healthy control animals (767 up regulated, 418 down regulated). These genes were grouped by K-means clustering into seven distinct transcriptional patterns, and the predominant biological processes represented by the genes in each cluster were identified (Fig. 4).

As expected, immune response-associated and defense response-associated gene families dominated the list of genes up regulated in SIV-infected macaques independent of ART (clusters 3 and 4). Additional biological processes or pathways that were significantly up regulated in all SIV-infected animals included proteolysis (ubiquitination based), RNA processing, energy derivation, and antigen presentation. Genes down regulated in SIV-infected macaques, independent of ART (clusters 6 and 7), included those involved in ion channel structure and activity, synaptic transmission, transcriptional regulation, calmodulin binding, and ligase activity.

The differences in gene expression between PMPA-treated and untreated SIV-infected macaques are shown in clusters 1, 2, and 5. Cluster 1 depicts genes up regulated only in untreated SIV-infected macaques and contains a significant number of additional defense response-associated genes not shown in cluster 3 or 4, as well as genes involved in protein biosynthesis, proteolysis, cell cycle regulation, and response to oxidative stress. Cluster 5 depicts genes down regulated exclusively in untreated SIV-infected animals, which included genes associated with transcription, ATP binding, protein catabolism, calmodulin binding, and ligase activity. Interestingly, cluster 2, showing genes up regulated only in PMPA-treated SIV-infected macaques, included significant numbers of transcripts involved in organogenesis as well as protein catabolism, energy derivation, transport, and cell adhesion. Given that the most prominent functional categories identified through the clustering and ontology analyses (i.e., defense response and organogenesis) also reflected the potential mechanisms and downstream effects of intestinal $CD4^+$ T-cell depletion and reconstitution, we focused our gene expression analysis on characterizing changes in transcription associated with defense response and mucosal regeneration in PMPA-treated and untreated animals.

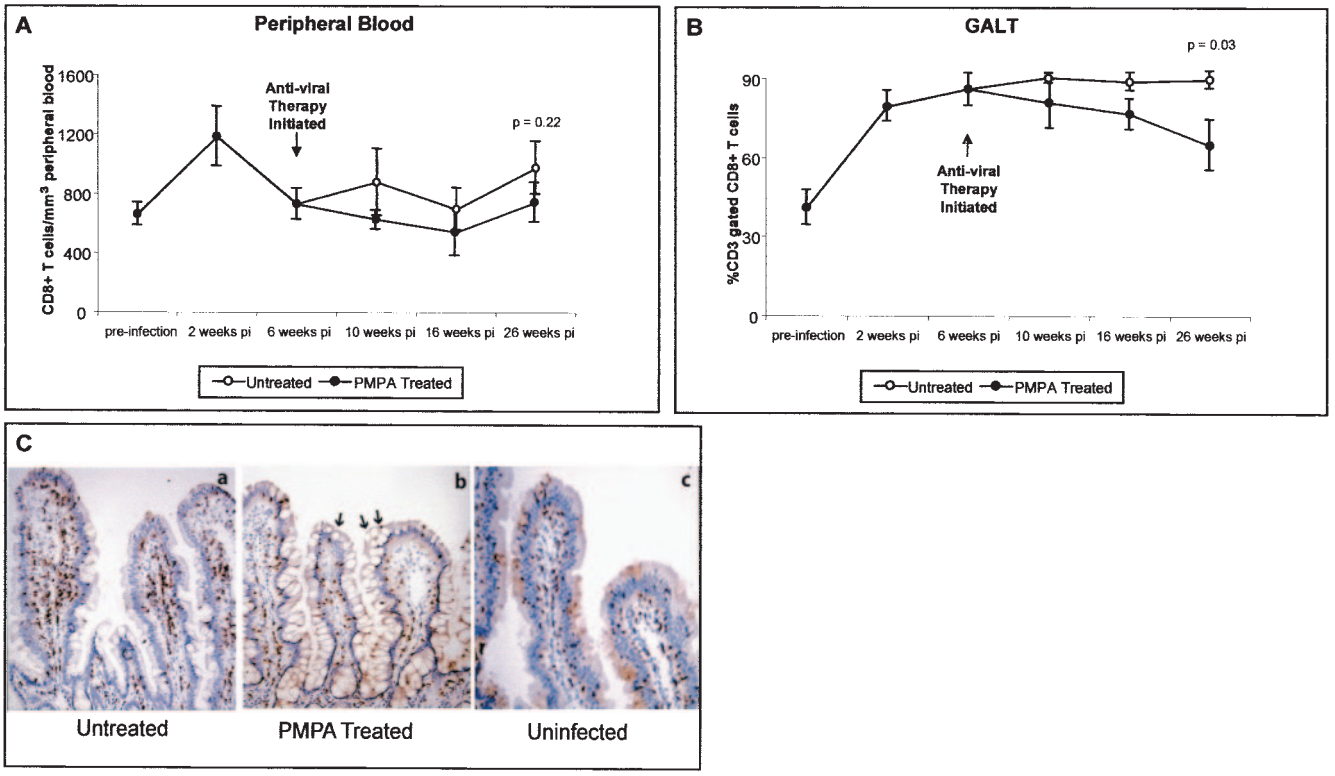

FIG. 3. Reduced $CD8^+$ T lymphocytosis in PMPA-treated SIV-infected macaques. The levels of $CD8^+$ T cells in peripheral blood (A) and the gastrointestinal mucosa (B and C) were determined prior to SIV infection and monitored in treated and untreated macaques at the indicated time points by flow cytometry (A and B) and by immunohistochemistry (C) at 26 weeks p.i. Direct counting revealed an increase in $CD8^+$ T cells in GALT in untreated SIV-infected animals (C, panel a) compared to SIV-infected macaques undergoing ART (b) and healthy uninfected controls (c). An increase in goblet cells was also observed in PMPA-treated SIV-infected animals (b).

Increased expression of inflammatory response and lymphocyte activation-associated genes in untreated SIV infection. To comprehensively characterize the differences in defense response-associated expression in GALT of untreated and PMPA-treated SIV-infected macaques, we first assigned genes within this broad functional family into more specific categories (Fig. 5). The number and proportion of genes involved in lymphocyte activation and inflammatory responses was substantially higher in the untreated group compared to the PMPA-treated group (Fig. 5A). Expression of IL-5, RANTES, CXCL11, phospholipase D1, annexin A1, and eight other stress-associated or inflammatory response-associated genes was increased only in untreated SIV-infected macaques (Fig. 5B). Additionally, we found that granzymes A and B, superoxide dismutase 2, catalase, and dual specificity phosphatase 1 were also up regulated only in the untreated SIV-infected animals. These data suggested that the increased prevalence of mucosal $CD8^+$ T cells may have contributed to the elevated expression of genes associated with inflammation and high levels of localized granzyme-induced killing.

In addition to proinflammatory factors, untreated SIV-infected macaques also displayed increased expression of several well-known mediators of immune cell activation in GALT (Fig. 5B). In contrast to the PMPA-treated macaques, IL-15, signal transducer and activator of transcription (STAT) 1 and 2, and CREB binding protein (CREBP) were all increased exclusively in the untreated macaques, suggesting that signaling and activation within the mucosal immune system may have been chronically elevated in untreated SIV-infected animals. Additionally, Notch 1 homologue and colony stimulating factor receptor 2 (CSFR-2) were up regulated exclusively in the untreated macaques, suggesting a potential for increased presence of activated macrophages and dendritic cells, respectively, within the intestinal mucosa during chronic SIV infection.

Antigen presentation and humoral immune response-associated genes are up regulated in SIV infection independent of therapy. In contrast to the divergent expression profiles observed in inflammatory response and immune cell activation between the treated and untreated groups, acquired and innate immunity-associated genes were, in general, up regulated in all SIV-infected animals. Transcription of genes involved in antigen presentation, including major histocompatibility complex class I (MHC I) A, B, C, and F, and MHC II DMA, DOA, DPB1, DQA1, DQB1, DRB1, DRB3, DRB4, and DRB6, was elevated in both PMPA-treated and untreated macaques (Fig. 5C). Genes involved in ubiquitin-dependent protein degradation were also up regulated in all SIV-infected animals, including various proteasome subunits and ubiquitin-specific carriers and enzymes, indicating that antigen processing and presentation in GALT were activated. We also found that IgM, -G, -L, and -K were substantially up regulated in both untreated and PMPA-treated macaques, suggesting that B-cell responses were not inhibited in GALT during chronic SIV infection nor down regulated in animals receiving antiviral therapy.

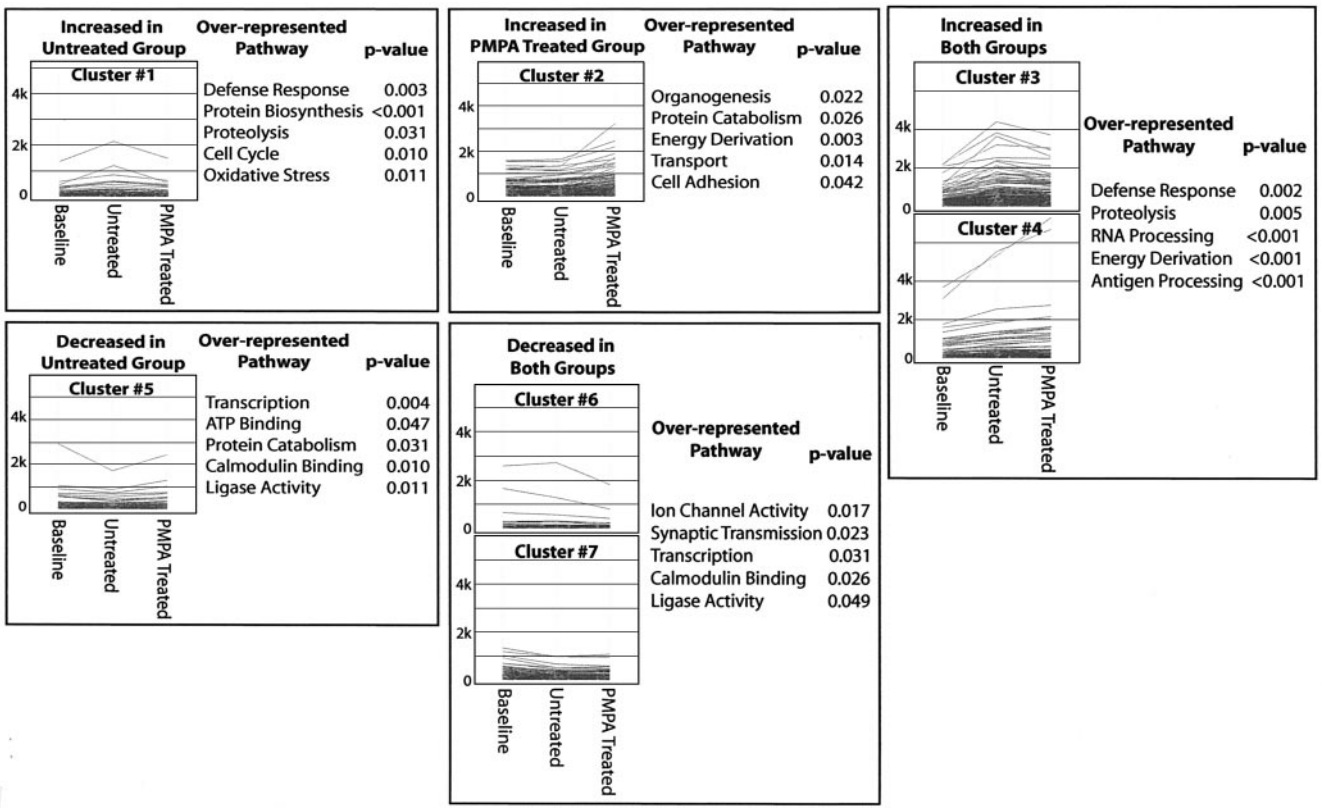

FIG. 4. Gene expression profiling of the host response to SIV infection. Average mRNA levels in healthy GALT were determined by microarray analyses of six uninfected control samples and compared to the average mRNA levels after 26 weeks in untreated or PMPA-treated SIV-infected animals. Genes whose expression was regulated by at least 50% (up or down) in a majority of macaques ($P < 0.05$) within each experimental group were identified and subjected to K-means clustering, followed by categorization of the genes in each cluster into physiological functions. Fluorescence intensity values are shown on the *y* axis for each cluster, and mean intensities for uninfected, untreated SIV-infected, and PMPA-treated SIV-infected groups are plotted. Biological processes and pathways statistically overrepresented ($P < 0.05$) by the genes in each cluster were identified through GO ontology analysis as described in Materials and Methods. The top five biological processes represented by the data in each cluster are shown.

To provide validation for transcriptional data generated by microarray analysis, we examined expression of RANTES, MIP-1β, and granzyme A by real-time PCR and expression of IgG by immunohistochemistry. Increased levels of RANTES, MIP-1β, and granzyme A transcripts were detected at 26 weeks p.i. in untreated animals in comparison to PMPA-treated macaques (Fig. 6A), confirming the results of DNA microarray analysis (Fig. 5). Additionally, immunohistochemistry analysis demonstrated that levels of IgG protein in GALT were substantially increased in untreated SIV-infected animals compared to PMPA-treated macaques, indicating that increases in transcription detected by microarray analysis corresponded to increases in protein levels (Fig. 6B).

Mucosal epithelial growth and repair-associated gene expression is enhanced in SIV-infected macaques receiving ART. Our previous studies have demonstrated that SIV infection can lead to impaired barrier and absorptive functions of intestinal epithelium (8). To evaluate the molecular changes associated with repair and maintenance of mucosal barrier functions caused by SIV infection and antiviral therapy, expression of genes involved in the trefoil factor 3 (TFF3)-mediated pathway of intestinal epithelial regeneration was analyzed (Fig. 7A). Expression of TFF3, integrin β1, epidermal growth factor receptor, mucin 2, phosphoinositide-3-kinase, Bcl-2 antagonist of cell death (BAD), and various cell-cell and cell-substratum adhesion molecules (listed in Fig. 7B) was up regulated in GALT of PMPA-treated SIV-infected macaques, while only BAD and mucin-2 were up regulated in untreated animals. These data suggested that mucosal repair mechanisms may have been impaired in SIV-infected animals in the absence of therapy. This conclusion was further supported by the observation that substantially more mucin-2 was expressed in PMPA-treated macaques (3.4- versus 1.5-fold increase). The reduction of TFF3 and mucin-2 expression in untreated macaques also coincided with down regulation of mitogen-activated protein kinase 1 (erk-1), implying that inhibition of transcription may have involved attenuation of mitogen-activated protein kinase signaling, possibly due to changes in the make up of the resident T-cell subsets.

To determine if the reduced expression of genes regulating intestinal epithelial repair and maintenance was associated with dysregulation of genes involved in enterocyte function, we examined changes in several digestion-associated transcripts as markers of enterocyte differentiation, maturation, and function (Fig. 8). In SIV-infected macaques receiving ART, we found consistent up regulation of genes encoding digestive enzymes

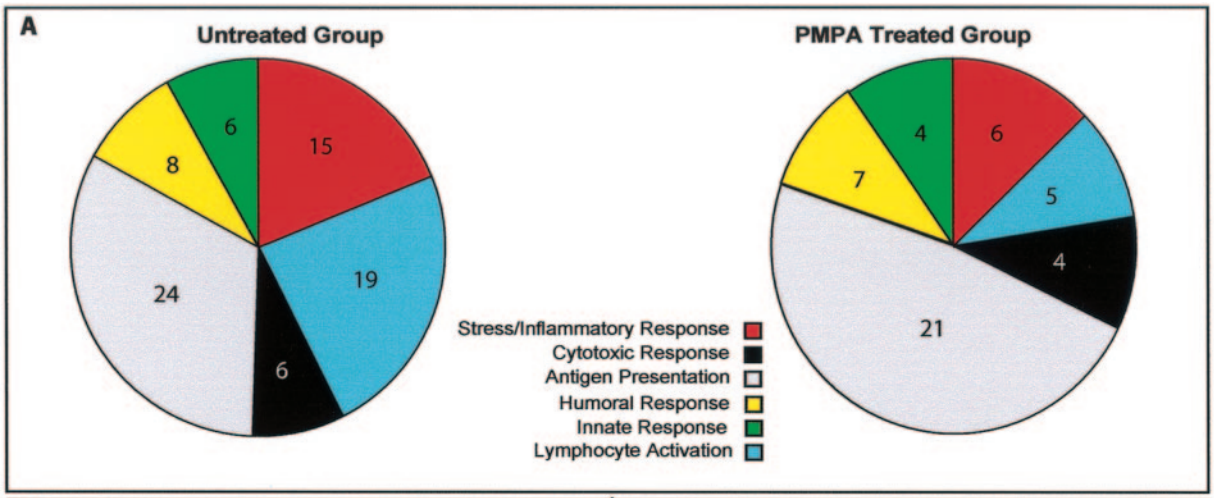

B

Stress/Inflammatory Response

Untreated	PMPA Treated
stress-induced-phosphoprotein 1	stress-induced-phosphoprotein 1
Microsomal Glutathione-S-Transferase 2	Microsomal Glutathione-S-Transferase 2
Microsomal Glutathione-S-Transferase 3	Microsomal Glutathione-S-Transferase 3
Macrophage migration inhibitory factor	Macrophage migration inhibitory factor
Proteoglycan 1	Proteoglycan 1
RANTES	
IL-5	
CXCL11	
Endoglycan	
Platelet activating factor receptor	
Serum Amyloid A2	
phospholipase D1	
dual specificity phosphatase 1	
guanylate binding protein 1	
Tryptase, alpha	
Nexin	
Tissue factor pathway inhibitor 2	
superoxide dismutase 2	
pancreatitis-associated protein	
Catalase	
Annexin A1	
Crystalin, alpha A	

Lymphocyte Activation

Untreated	PMPA Treated
Interferon regulatory factor 3	Interferon regulatory factor 3
Interferon stimulated gene 20kDa	Interferon stimulated gene 20kDa
CD86 antigen	CD86 antigen
Dipeptidylpeptidase 4/CD26	Dipeptidylpeptidase 4/CD26
NFAT	NFAT
Protein tyrosine kinase binding protein	Protein tyrosine kinase binding protein
CDP-diacylglycerol synthase 1	
Colony stimulating factor 2	
Notch 1 homolog	
STAT-1	
STAT2	
CREBP	
T cell receptor beta	
IL-15	
IFN alpha-inducible protein (IFI-6-16)	

Cytotoxic Response

Untreated	PMPA Treated
HLA-A	HLA-A
HLA-B	HLA-B
HLA-C	HLA-C
HLA-F	HLA-F
Granzyme A	
Granzyme B	

C

Humoral Response

Untreated	PMPA Treated
Cysteine-rich protein 1	Cysteine-rich protein 1
Immunoglobulin heavy constant gamma 3	Immunoglobulin heavy constant gamma 3
Immunoglobulin heavy constan mu	Immunoglobulin heavy constan mu
Immunoglobulin lambda joining 3	Immunoglobulin lambda joining 3
Immunoglobulin lambda	Immunoglobulin lambda
immunoglobulin kappa constant	immunoglobulin kappa constant
Lymphocyte-specific protein 1	immunoglobulin kappa constant
Pre-B lymphocyte gene 1	

Antigen Presentation

Untreated	PMPA Treated
CD74 antigen	CD74 antigen
HLA-DMA	HLA-DMA
HLA-DOA	HLA-DOA
HLA-DPB1	HLA-DPB1
HLA-DQA1	HLA-DQA1
HLA-DQB1	HLA-DQB1
HLA-DRB1	HLA-DRB1
HLA-DRB3	HLA-DRB3
HLA-DRB4	HLA-DRB4
HLA-DRB6	HLA-DRB6
proteasome 26S subunit, ATPase, 6	proteasome 26S subunit, ATPase, 6
proteasome 26S subunit, non-ATPase, 11	proteasome 26S subunit, non-ATPase, 11
proteasome subunit, beta type, 10	proteasome subunit, beta type, 10
proteasome subunit, beta type, 2	proteasome subunit, beta type, 2
proteasome subunit, beta type, 3	proteasome subunit, beta type, 3
proteasome subunit, beta type, 9	proteasome subunit, beta type, 9
ubiquitin carrier protein	ubiquitin carrier protein
ubiquitin specific protease 1	ubiquitin specific protease 1
ubiquitin specific protease 16	ubiquitin specific protease 16
ubiquitin-conjugating enzyme E2D 3	ubiquitin-conjugating enzyme E2D 3
ubiquitin-conjugating enzyme E2M	ubiquitin-conjugating enzyme E2M
CD1E antigen	
Leukocyte immunoglobulin-like receptor	
Nuclease sensitive element binding protein 1	

Innate Response

Untreated	PMPA Treated
Complement component 1, alpha	Complement component 1, alpha
Complement component 1, beta	Complement component 1, beta
Complement component 1, binding protein	Complement component 1, binding protein
Complement component 2	Complement component 2
defensin, alpha 6, Paneth cell-specific	
interferon, omega 1	

FIG. 5. Categorization of up regulated defense response-associated gene expression in SIV-infected macaques. (A) Pie chart depicting proportions of up regulated genes in both PMPA-treated and untreated SIV-infected animals involved in specific categories of the host response in GALT. The number of genes in each category is shown. (B and C) Genes up regulated in GALT in SIV-infected macaques and associated with the host defense response (depicted in the pie charts in panel A). Genes shown in both PMPA treated and untreated columns were up regulated in both groups, while genes listed in only one of the columns were up regulated exclusively within that group.

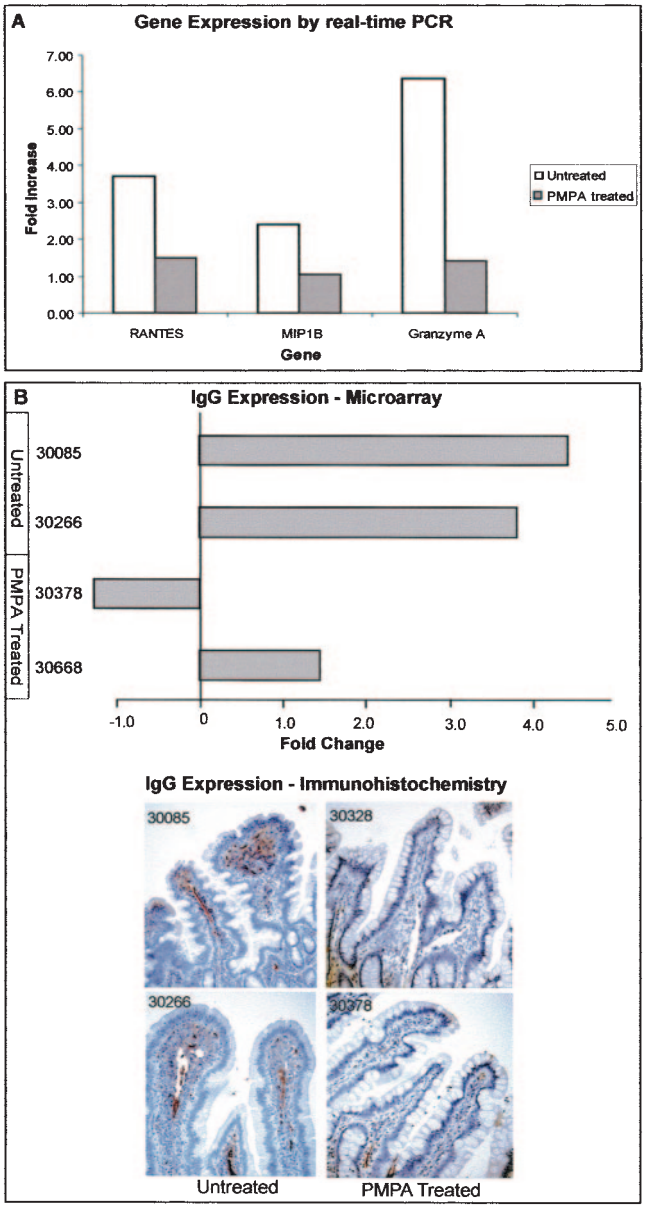

FIG. 6. Validation of microarray data by real-time PCR and immunohistochemistry. (A) In agreement with the microarray analysis shown in Fig. 6, real-time PCR indicated that transcription of RANTES, MIP-1β, and granzyme A was increased only in untreated SIV-infected macaques. Changes in expression are shown as mean fold changes for each group. (B) Increased expression of IgG was detected in untreated SIV-infected macaques (30085 and 30266) by both microarray and immunohistochemistry analyses, in comparison to the level of expression in PMPA-treated SIV-infected animals (30668 and 30378).

(sucrase-isomaltase and maltase glucoamylase) and molecules associated with stimulation of feeding behavior (glucagon, peptide YY, and cholecystokinin receptor A). We concluded that increased transcription of these genes only in PMPA-treated macaques provided supportive evidence of restoration of mucosal tissue by growth and regeneration of the mucosal epithelium in comparison to untreated SIV-infected macaques.

DISCUSSION

Previous studies have indicated that GALT is an early target organ for both HIV-1 and SIV replication and a site of severe $CD4^+$ T-cell depletion during primary viral infection (4, 6, 8, 12, 17, 29, 39). Administration of HAART has been shown to effectively suppress HIV-1 replication and increase $CD4^+$ T cells in peripheral blood and GALT (2, 6, 9, 32) and results in a decreased number of cases progressing to AIDS (2). A recent report indicated that initiation of HAART during primary HIV-1 infection led to near-complete restoration of $CD4^+$ T cells in the intestinal mucosa, while starting therapy during chronic HIV-1 infection resulted in substantially delayed and incomplete mucosal $CD4^+$ T-cell restoration (6). In the SIV model, the clinical benefits of PMPA therapy have been shown to include enhanced immune response (30), improved repopulation of peripheral $CD4^+$ T cells (16, 26, 30, 31, 34), and increased survival rates (37). Our investigation has provided additional insight, demonstrating that the initiation of PMPA therapy during early SIV infection (6 weeks p.i.) led to a dramatic reduction in mucosal viral loads (Fig. 1) and an efficient restoration of $CD4^+$ T cells in both GALT and peripheral blood (Fig. 2). Future studies focused on functional characterization of repopulating intestinal $CD4^+$ T cells during SIV and HIV infection remain warranted, however, especially in light of previous investigations suggesting potential defects in cytokine production (16).

While numerous reports indicate that the onset of dysregulation of mucosal immune system and digestive functions may often occur during early stages of HIV and SIV infection (8, 11–14), the molecular bases of these intestinal mucosal pathologies have not been fully investigated. Functional genomic analysis has provided comprehensive evidence of dysregulated gene expression in the TFF3 pathway in GALT of SIV-infected animals (Fig. 7). Mucin-2 and TFF3, as well as genes encoding receptors, signaling molecules, and structural proteins involved in intestinal epithelial growth and repair, were expressed at substantially higher levels in PMPA-treated than in untreated SIV-infected macaques (Fig. 7B), indicating that epithelial growth and repair may have been impaired in untreated animals with high mucosal viral burdens. These data were supported by histological analysis that highlighted a substantial increase in the number of goblet cells in the jejunal epithelium of treated animals (Fig. 3C). TFF-3 is known to be secreted by goblet cells and enterocytes within the intestinal mucosa, providing cytoprotective function as well as direct stimulus for epithelial growth and repair (33). It is also noteworthy that exogenous TFF3 has been shown to provide some therapeutic benefit in studies of enterocolitis in the mouse model (42). Interestingly, we have detected down regulation of TFF expression in GALT during primary SIV infection as early as 2 weeks p.i. (data not shown), indicating that disruption of epithelial growth and repair may be an early enteropathogenic mechanism of SIV infection, preceding the onset of detectable morphological changes, and may adversely affect the restoration of mucosal structure and function.

Increased immune activation in GALT following SIV infection may contribute to mucosal barrier damage through up regulation of multiple cytokines and chemokines that can also stimulate inflammatory response and cell death (7, 11, 19, 25).

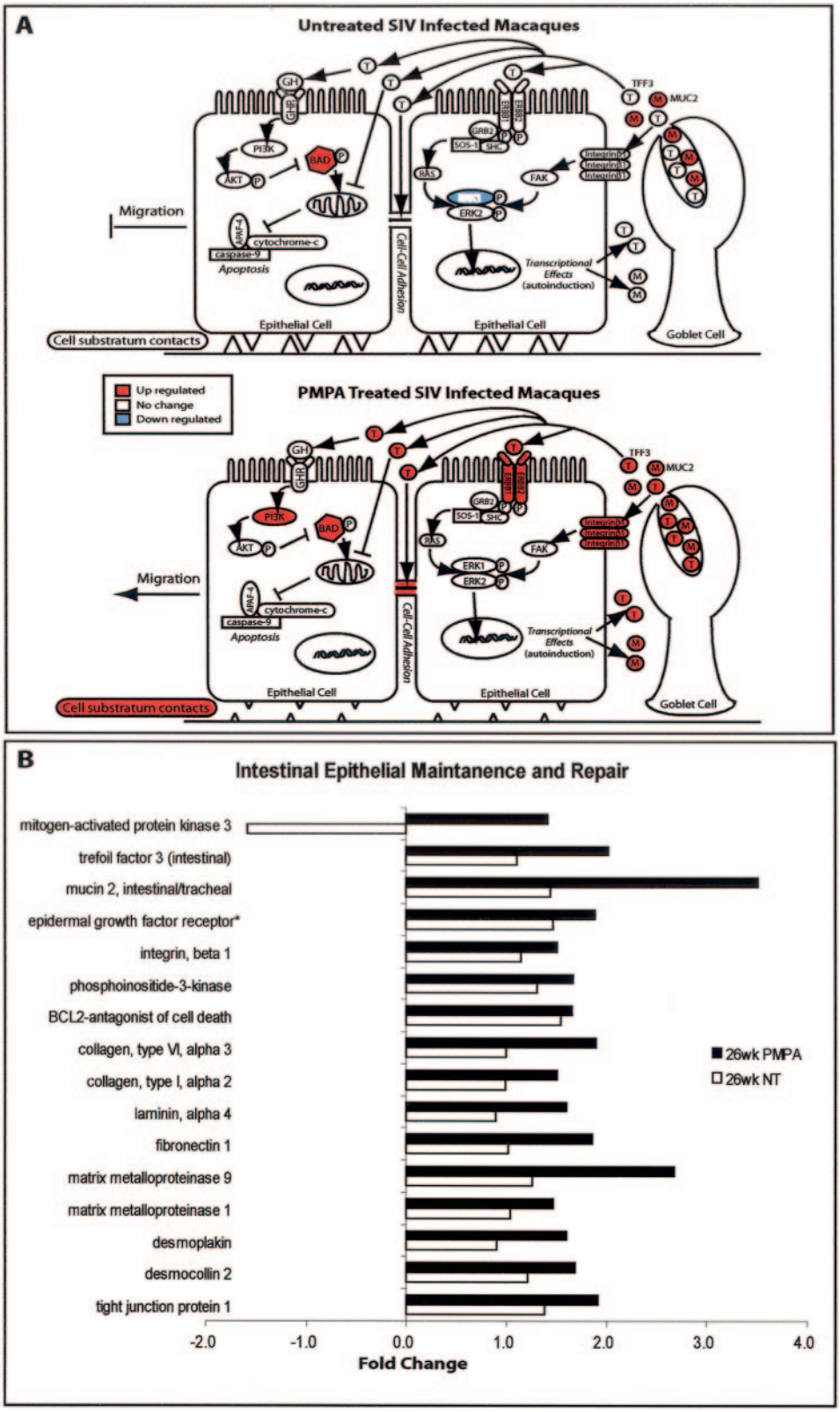

FIG. 7. Up regulation of genes mediating intestinal epithelial growth and repair in SIV-infected macaques receiving ART. (A) Changes in expression of genes involved in TFF3-mediated intestinal epithelial repair and maintenance are shown as up regulated (red), down regulated (blue), or not changing (white) in both PMPA-treated and untreated SIV-infected groups. (B) Changes in mucosal epithelial repair and maintenance-associated genes were plotted for each gene in the pathway regulated by at least 1.5-fold in untreated (white bars) and PMPA-treated (black bars) SIV-infected animals. *, $P > 0.05$ versus untreated.

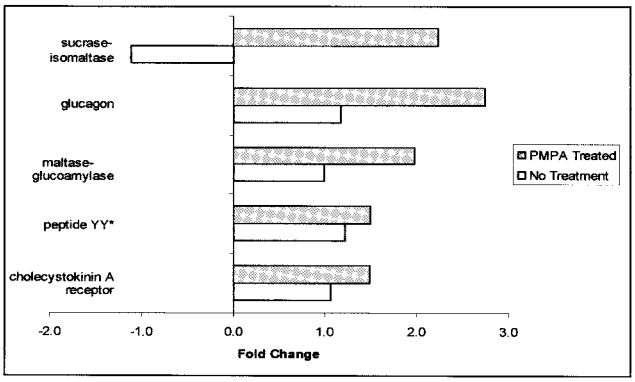

FIG. 8. Expression of genes associated with digestive processes is enhanced in PMPA-treated SIV-infected macaques. Changes in the levels of transcription of digestion-associated genes were determined by microarray analysis in PMPA-treated (gray bars) and untreated (white bars) SIV-infected animals.

The mucosal gene expression profiles of chronically SIV-infected animals in our studies strongly supported this hypothesis. A substantial increase in the expression of genes regulating stress and inflammatory responses (RANTES, IL-5, CXCL11, SOD-2, catalase, annexin A1, etc.) and immune activation (IL-15, STAT-1, STAT-2, CSF-2, etc.) was observed in untreated SIV-infected macaques in comparison to PMPA-treated animals (Fig. 5). Additionally, we found that expression of activation markers for macrophages (Notch 1 homologue) and dendritic cells (CSFR-2) was also increased exclusively in untreated SIV-infected animals, suggesting a broad range of immune activation in GALT. These data also support findings in previous HIV-1 studies that have reported intestinal mucosal inflammation and increased expression of proinflammatory cytokines and chemokines (21). Recently, gene expression profiling of lymph node biopsies from HIV-1-infected patients also indicated that immune activation pathways were highly up regulated in the absence of HAART, while patients receiving HAART displayed significant up regulation of genes involved in tissue repair and cell trafficking (23). These studies supply both molecular and histological evidence that increased lymphocyte activation and inflammation may play a key role in the manifestation of gastrointestinal pathologies associated with HIV and SIV infection.

Taken together, our investigation and previous reports suggest that therapeutic strategies to reduce the level of inflammation and increase mucosal growth and injury repair should be investigated to enhance the efficacy of anti-HIV or -SIV therapy in restoring mucosal immune system. Down regulation of lymphocyte activation during HIV infection has been proposed by several investigators as a potential method to improve the rate of disease progression (3, 5, 17, 24). It is also noteworthy that inhibitors of tumor necrosis factor have been shown to markedly reduce mucosal inflammation caused by infection of intestinal xenografts, suggesting that tumor necrosis factor-associated pathways may play an important role in the manifestation of intestinal inflammation in HIV and SIV infections (43). Recently, administration of human growth hormone in patients receiving HAART was shown to improve T-cell maturation and function (22), suggesting that addition of growth supplements in HAART regimens can potentially improve clinical outcome. Therapeutic strategies that induce intestinal epithelial growth and repair may also serve to delay disease progression by enhancing nutrient absorption and barrier integrity through better maintenance of mucosal structure and function. Our studies suggest that the TFF3 pathway mediating epithelial growth and repair could provide potential molecular targets to investigate novel therapeutic approaches to restore intestinal mucosal function during SIV and HIV infections.

The intestinal mucosal expression profiles we have elucidated provide a novel in vivo snapshot of the biological processes modulated by SIV infection and those restored by ART. Monitoring host gene expression in these processes may provide opportunities to identify potential molecular correlates of enteropathogenesis as well as diverse clinical outcomes. Future studies that identify and characterize transcriptional profiles of specific isolated mucosal cell subtypes from long-term survivors to those of rapid progressors and patients failing therapy will be especially important in the precise identification of molecular markers of enteropathogenesis as well as putative therapeutic targets.

ACKNOWLEDGMENTS

We thank Linda Hirst and the animal care technicians at the Northern California National Primate Research Center for their hard work and dedication, Thomas Ndolo and Angie Gelli for their review of the manuscript, and Melanie Silvey and the Lucy Whittier Molecular Core Facility for their technical support.

This study was supported by grants from the National Institutes of Health (DK-43183, AI-43274) and the Northern California Center for AIDS Research (PHS-AI49366).

REFERENCES

1. **Bell, D. J., and D. H. Dockrell.** 2003. Apoptosis in HIV-1 infection. J. Eur. Acad. Dermatol. Venereol. **17:**178–183.
2. **Brigido, L., R. Rodrigues, J. Casseb, R. M. Custodio, L. A. Fonseca, M. Sanchez, and A. J. Duarte.** 2004. $CD4^+$ T-cell recovery and clinical outcome in HIV-1-infected patients exposed to multiple antiretroviral regimens: partial control of viremia is associated with favorable outcome. AIDS Patient Care STDs. **18:**189–198.
3. **Galati, D., M. Bocchino, M. Paiardini, B. Cervasi, G. Silvestri, and G. Piedimonte.** 2002. Cell cycle dysregulation during HIV infection: perspectives of a target based therapy. Curr. Drug Targets Immune Endocr. Metabol. Disord. **2:**53–61.
4. **George, M. D., S. Sankaran, E. Reay, A. C. Gelli, and S. Dandekar.** 2003. High-throughput gene expression profiling indicates dysregulation of intestinal cell cycle mediators and growth factors during primary simian immunodeficiency virus infection. Virology **312:**84–94.
5. **Gougeon, M. L., and L. Montagnier.** 1999. Programmed cell death as a mechanism of CD4 and CD8 T cell deletion in AIDS. Molecular control and effect of highly active anti-retroviral therapy. Ann. N. Y. Acad. Sci. **887:**199–212.
6. **Guadalupe, M., E. Reay, S. Sankaran, T. Prindiville, J. Flamm, A. McNeil, and S. Dandekar.** 2003. Severe $CD4^+$ T-cell depletion in gut lymphoid tissue during primary human immunodeficiency virus type 1 infection and substantial delay in the restoration following highly active antiretroviral therapy. J. Virol. **77:**11708–11717.
7. **Gummuluru, S., F. J. Novembre, M. Lewis, H. A. Gelbard, and S. Dewhurst.** 1996. Apoptosis correlates with immune activation in intestinal lymphoid tissue from macaques acutely infected by a highly enteropathic simian immunodeficiency virus, $SIV_{smmPBj14}$. Virology **225:**21–32.
8. **Heise, C., C. J. Miller, A. Lackner, and S. Dandekar.** 1994. Primary acute simian immunodeficiency virus infection of intestinal lymphoid tissue is associated with gastrointestinal dysfunction. J. Infect. Dis. **169:**1116–1120.
9. **Hirsch, H. H., G. Kaufmann, P. Sendi, and M. Battegay.** 2004. Immune reconstitution in HIV-infected patients. Clin. Infect. Dis. **38:**1159–1166.
10. **Hosack, D. A., G. Dennis, Jr., B. T. Sherman, H. C. Lane, and R. A. Lempicki.** 2003. Identifying biological themes within lists of genes with EASE. Genome Biol. **4:**P4.
11. **Kaup, F., K. Matz-Rensing, E. Kuhn, P. Hunerbein, C. Stahl-Hennig, and G.**

Hunsmann. 1998. Gastrointestinal pathology in rhesus monkeys with experimental SIV infection. Pathobiology **66:**159–164.
12. **Kewenig, S., T. Schneider, K. Hohloch, K. Lampe-Dreyer, R. Ullrich, N. Stolte, C. Stahl-Hennig, F. J. Kaup, A. Stallmach, and M. Zeitz.** 1999. Rapid mucosal CD4$^+$ T-cell depletion and enteropathy in simian immunodeficiency virus-infected rhesus macaques. Gastroenterology **116:**1115–1123.
13. **Kotler, D. P.** 1999. Characterization of intestinal disease associated with human immunodeficiency virus infection and response to antiretroviral therapy. J Infect. Dis. **179**(Suppl. 3)**:**S454–S456.
14. **Kotler, D. P., S. Reka, and F. Clayton.** 1993. Intestinal mucosal inflammation associated with human immunodeficiency virus infection. Dig. Dis. Sci. **38:** 1119–1127.
15. **Mattapllil, J. J., E. Reay, and S. Dandekar.** 2000. An early expansion of CD8$\alpha\beta$ T cells, but depletion of resident CD8$\alpha\alpha$ T cells, occurs in the intestinal epithelium during primary simian immunodeficiency virus infection. AIDS **14:**637–646.
16. **Mattapallil, J. J., Z. Smit-McBride, P. Dailey, and S. Dandekar.** 1999. Activated memory CD4$^+$ T helper cells repopulate the intestine early following antiretroviral therapy of simian immunodeficiency virus-infected rhesus macaques but exhibit a decreased potential to produce interleukin-2. J. Virol. **73:**6661–6669.
17. **McCune, J. M.** 2001. The dynamics of CD4$^+$ T cell depletion in HIV disease. Nature **410:**974–979.
18. **McGowan, I., G. Radford-Smith, and D. P. Jewell.** 1994. Cytokine gene expression in HIV-infected intestinal mucosa. AIDS **8:**1569–1575.
19. **Ndolo, T., J. Rheinhardt, M. Zaragoza, Z. Smit-McBride, and S. Dandekar.** 1999. Alterations in RANTES gene expression and T-cell prevalence in intestinal mucosa during pathogenic or nonpathogenic simian immunodeficiency virus infection. Virology **259:**110–118.
20. **Oktedalen, O., V. Skar, E. Dahl, and A. Serck-Hanssen.** 1998. Changes in small intestinal structure and function in HIV-infected patients with chronic diarrhoea. Scand. J. Infect. Dis. **30:**459–463.
21. **Olsson, J., M. Poles, A. L. Spetz, J. Elliott, L. Hultin, J. Giorgi, J. Andersson, and P. Anton.** 2003. Human immunodeficiency virus type 1 infection is associated with significant mucosal inflammation characterized by increased expression of CCR5, CXCR4, and beta-chemokines. J. Infect. Dis. **182:**1625–1635.
22. **Pires, A., J. Pido-Lopez, G. Moyle, B. Gazzard, F. Gotch, and N. Imami.** 2004. Enhanced T-cell maturation, differentiation and function in HIV-1-infected individuals after growth hormone and highly active antiretroviral therapy. Antivir. Ther. **9:**67–75.
23. **Qingsheng, L., T. Schacker, J. Carlis, G. Beilman, P. Nguyen, and A. T. Haase.** 2004. Functional genomic analysis of the response of HIV-1-infected lymphatic tissue to antiviral therapy. J. Infect. Dis. *18***9:**572–582.
24. **Regulier, E. G., K. Reiss, K. Khalil, S. Amini, J. Rappaport, J. F. Zagury, and P. D. Katsikis.** 2004. T-cell and neuronal apoptosis in HIV infection: implications for therapeutic intervention. Int. Rev. Immunol. **23:**25–59.
25. **Reinhart, T. A., B. A. Fallert, M. E. Pfeifer, S. Sanghavi, S. Capuano III, P. Rajakumar, M. Murphey-Corb, R. Day, C. L. Fuller, and T. M. Schaefer.** 2002. Increased expression of the inflammatory chemokine CXC chemokine ligand 9/monokine induced by interferon-gamma in lymphoid tissues of rhesus macaques during simian immunodeficiency virus infection and acquired immunodeficiency syndrome. Blood **99:**3119–3128.
26. **Rosenwirth, B., P. ten Haaft, W. M. Bogers, I. G. Nieuwenhuis, H. Niphuis, E. M. Kuhn, N. Bischofberger, J. L. Heeney, and K. Uberla.** 2000. Antiretroviral therapy during primary immunodeficiency virus infection can induce persistent suppression of virus load and protection from heterologous challenge in rhesus macaques. J. Virol. **74:**1704–1711.
27. **Sabri, F., K. Titanji, A. De Milito, and F. Chiodi.** 2003. Astrocyte activation and apoptosis: their roles in the neuropathology of HIV infection. Brain Pathol. **13:**84–94.
28. **Schmitz, J. E., M. J. Kuroda, R. S. Veazey, A. Seth, W. M. Taylor, C. E. Nickerson, M. A. Lifton, P. J. Dailey, M. A. Forman, P. Racz, K. Tenner-Racz, and N. L. Letvin.** 2000. Simian immunodeficiency virus (SIV)-specific CTL are present in large numbers in livers of SIV-infected rhesus monkeys. J. Immunol. **164:**6015–6019.
29. **Smit-McBride, Z., J. J. Mattapallil, M. McChesney, D. Ferrick, and S. Dandekar.** 1998. Gastrointestinal T lymphocytes retain high potential for cytokine responses but have severe CD4$^+$ T-cell depletion at all stages of simian immunodeficiency virus infection compared to peripheral lymphocytes. J. Virol. **72:**6646–6656.
30. **Smith, M. S., L. Foresman, G. J. Lopez, J. Tsay, D. Wodarz, J. D. Lifson, A. Page, C. Wang, Z. Li, I. Adany, S. Buch, N. Bischofberger, and O. Narayan.** 2000. Lasting effects of transient postinoculation tenofovir [9-*R*-(2-phosphonomethoxypropyl)adenine] treatment on SHIV(KU2) infection of rhesus macaques. Virology **277:**306–315.
31. **Spring, M., C. Stahl-Hennig, N. Stolte, N. Bischofberger, J. Heeney, P. ten Haaft, K. Tenner-Racz, P. Racz, D. Lorenzen, G. Hunsmann, and U. Dittmer.** 2001. Enhanced cellular immune response and reduced CD8$^+$ lymphocyte apoptosis in acutely SIV-infected rhesus macaques after short-term antiretroviral treatment. Virology **279:**221–232.
32. **Talal, A. H., S. Monard, M. Vesanen, Z. Zheng, A. Hurley, Y. Cao, F. Fang, L. Smiley, J. Johnson, R. Kost, and M. H. Markowitz.** 2001. Virologic and immunologic effect of antiretroviral therapy on HIV-1 in gut-associated lymphoid tissue. J. Acquir. Immune Defic. Syndr. **26:**1–7.
33. **Taupin, D., and D. K. Podolsky.** 2003. Trefoil factors: initiators of mucosal healing. Nat. Rev. Mol. Cell Biol. **4:**721–732.
34. **Tsai, C. C., K. E. Follis, T. W. Beck, A. Sabo, N. Bischofberger, and P. J. Dailey.** 1997. Effects of (*R*)-9-(2-phosphonylmethoxypropyl)adenine monotherapy on chronic SIV infection in macaques. AIDS Res. Hum. Retrovir. **13:**707–712.
35. **Ullrich, R., M. Zeitz, M. Heise, M. l'Age, G. Hofken, and E. O. Riecken.** 1989. Small intestinal structure and function in patients infected with human immunodeficiency virus (HIV): evidence for HIV-induced enteropathy. Ann. Intern. Med. **111:**15–21.
36. **Valdez, H.** 2002. Immune restoration after treatment of HIV-1 infection with highly active antiretroviral therapy (HAART). AIDS Rev. **4:**157–164.
37. **Van Rompay, K. K., R. P. Singh, L. L. Brignolo, J. R. Lawson, K. A. Schmidt, B. Pahar, D. R. Canfield, R. P. Tarara, D. L. Sodora, N. Bischofberger, and M. L. Marthas.** 2004. The clinical benefits of tenofovir for simian immunodeficiency virus-infected macaques are larger than predicted by its effects on standard viral and immunologic parameters. J. Acquir. Immune Defic. Syndr. **36:**900–914.
38. **Veazey, R. S., M. C. Gauduin, K. G. Mansfield, I. C. Tham, J. D. Altman, J. D. Lifson, A. A. Lackner, and R. P. Johnson.** 2001. Emergence and kinetics of simian immunodeficiency virus-specific CD8$^+$ T cells in the intestines of macaques during primary infection. J. Virol. **75:**10515–10519.
39. **Veazey, R. S., I. C. Tham, K. G. Mansfield, M. DeMaria, A. E. Forand, D. E. Shvetz, L. V. Chalifoux, P. K. Sehgal, and A. A. Lackner.** 2000. Identifying the target cell in primary simian immunodeficiency virus (SIV) infection: highly activated memory CD4$^+$ T cells are rapidly eliminated in early SIV infection in vivo. J. Virol. **74:**57–64.
40. **Vingert, B. C., R. Le Grand, and A. Venet.** 2003. Heterogeneity of the simian immunodeficiency virus (SIV) specific CD8$^+$ T-cell response in mucosal tissues during SIV primary infection. Microbes Infect. **5:**757–767.
41. **Zeitz, M., R. Ulrich, T. Schneider, S. Kewenig, and E. Riecken.** 1998. Mucosal immunodeficiency in HIV/SIV infection. Pathobiology **66:**151–157.
42. **Zhang, B. H., H. G. Yu, Z. X. Sheng, H. S. Luo, and J. P. Yu.** 2003. The therapeutic effect of recombinant human trefoil factor 3 on hypoxia-induced necrotizing enterocolitis in immature rat. Regul. Pept. **116:**53–60.
43. **Zhang, Z., S. Mahajan, X. Zhang, and S. L. Stanley, Jr.** 2003. Tumor necrosis factor alpha is a key mediator of gut inflammation seen in amebic colitis in human intestine in the SCID mouse-human intestinal xenograft model of disease. Infect. Immun. **71:**5355–5359.